Journal of Translational Autoimmunity 9 (2024) 100250

Contents lists available at ScienceDirect

Journal of Translational Autoimmunity

journal homepage: www.sciencedirect.com/journal/journal-of-translational-autoimmunity

Vascular injury derived apoptotic exosome-like vesicles trigger autoimmunity

Sandrine Juillard [a,b,c], Annie Karakeussian-Rimbaud [a], Marie-Hélène Normand [a,b,c], Julie Turgeon [a,c], Charlotte Veilleux-Trinh [a], Alexa C. Robitaille [a,b], Joyce Rauch [d], Andrzej Chruscinski [e], Nathalie Grandvaux [a,b], Éric Boilard [f], Marie-Josée Hébert [a,b,c,*], Mélanie Dieudé [a,b,c,g,**]

[a] Centre de Recherche Du Centre Hospitalier de l'Université de Montréal (CRCHUM), Tour Viger, R12.218, 900 Rue St-Denis, Montréal, QC, H2X 0A9, Canada
[b] Université de Montréal, 2900 Bd Édouard-Montpetit, Montréal, QC, H3T 1J4, Canada
[c] Canadian Donation and Transplantation Research Program (CDTRP), University of Alberta, Edmonton, AB, T6G 2E1, Canada
[d] Division of Rheumatology, Research Institute of the McGill University Health Centre (RI MUHC), 1001 Bd Décarie, Montréal, QC, H4A 3J1, Canada
[e] University of Toronto, 27 King's College Cir, Toronto, ON, M5S 1A1, Canada
[f] Centre de Recherche Du CHU de Québec, Université Laval, 2705 Bd Laurier, Québec, QC, G1V 4G2, Canada
[g] Medical Affairs and Innovation, Héma-Québec, 1070 Avenue des Sciences-de-la-Vie, Québec, QC, G1V 5C3, Canada

ARTICLE INFO

Handling editor: Y Renaudineau

Keywords:
ApoExos
Autoantibodies
Anti-LG3
Systemic lupus erythematosus (SLE)
Toll-like receptors (TLR)

ABSTRACT

According to a central tenet of classical immune theory, a healthy immune system must avoid self-reactive lymphocyte clones but we now know that B cells repertoire exhibit some level of autoreactivity. These autoreactive B cells are thought to rely on self-ligands for their clonal selection and survival. Here, we confirm that healthy mice exhibit self-reactive B cell clones that can be stimulated *in vitro* by agonists of toll-like receptor (TLR) 1/2, TLR4, TLR7 and TLR9 to secrete anti-LG3/perlecan. LG3/perlecan is an antigen packaged in exosome-like structures released by apoptotic endothelial cells (ApoExos) upon vascular injury. We demonstrate that the injection of ApoExos in healthy animals activates the IL-23/IL-17 pro-inflammatory and autoimmune axis, and produces several autoantibodies, including anti-LG3 autoantibodies and hallmark autoantibodies found in systemic lupus erythematosus. We also identify γδT cells as key mediators of the maturation of ApoExos-induced autoantibodies in healthy mice. Altogether we show that ApoExos released by apoptotic endothelial cells display immune-mediating functions that can stimulate the B cells in the normal repertoire to produce autoantibodies. Our work also identifies TLR activation and γδT cells as important modulators of the humoral autoimmune response induced by ApoExos.

1. Introduction

In contrast to the classical immune theory that a healthy immune system must avoid self-reactive lymphocyte clones, the normal B cell repertoire includes some autoreactive clones that may rely on self-ligands for their clonal selection and survival [1]. These humoral responses to autoantigens contribute significantly to autoimmune diseases [2–6].

Interestingly, a large part of immune homeostasis resides in the immune system's capacity to clear damaged and dying cells without triggering an immune response [6–8]. While apoptosis is a common non-immunogenic cell death mechanism, multiple autoantibodies directed against apoptotic antigens have been characterized in autoimmune diseases [9,10]. Given their morphological and molecular changes, apoptotic cells may drive the production of autoantigens. Thus, rapidly clearing apoptotic debris is crucial to maintaining immune tolerance [8,11].

Perlecan (LG3) is a proteoglycan found in the extracellular matrix of endothelial cells [12,13] that is released by apoptotic endothelial cells after caspase-3 activation. The LG3 fragment is contained in apoptotic exosome-like vesicles (ApoExos), which are extracellular membrane vesicles (diameter <100 nm, similar to exosomes) released by

* Corresponding author. Centre de recherche du CHUM (CRCHUM), Tour Viger, R12.412, 900 rue St-Denis, Montréal, QC, H2X 0A9, Canada.
** Corresponding author. Centre de recherche du CHUM (CRCHUM), Tour Viger, R12.436, 900 rue St-Denis, Montréal, QC, H2X 0A9, Canada.
E-mail addresses: marie-josee.hebert@umontreal.ca (M.-J. Hébert), melanie.dieude@umontreal.ca (M. Dieudé).

https://doi.org/10.1016/j.jtauto.2024.100250
Received 19 February 2024; Received in revised form 15 July 2024; Accepted 9 August 2024
Available online 11 August 2024

endothelial cells upon vascular injury [13,14]. ApoExos differ from classical apoptotic bodies and classical exosomes with respect to their size, protein content, biogenesis, and function [13–17]. We have previously extensively characterized ApoExos [13,18] and discovered their role in humoral autoimmune responses against LG3, as well as their involvement in graft rejection [13,15]. We also found that naïve mice exhibit a B cell memory response to LG3, suggesting that memory to LG3 is a normal response to the components of membrane vesicles released by apoptotic cells [16]. Furthermore, our observations suggest that a pro-inflammatory environment amplifies and modulates anti-LG3 humoral responses in ways that could modify their function and impact [12,13,16].

The functional importance of the sensors of inflammation that are toll like receptors (TLRs) in triggering autoimmune responses is gaining interest [19–21]. Indeed, circulating levels of TLR agonists are increased in multiple autoimmune conditions [22], and many TLRs have been linked to the pathophysiology of autoimmune diseases [21–26].

Here, we demonstrate that ApoExos released by apoptotic endothelial cells display immune-mediating functions that can stimulate the B cells in the normal repertoire to produce autoantibodies. Our work also identifies TLR activation and γδT cells as important modulators of the humoral autoimmune response induced by ApoExos.

2. Materials and methods

2.1. Endothelial cell culture and preparation of conditioned media

As previously described [13], murine endothelial cells (mECs) were isolated from the aorta of C57BL/6 mice (Wild Type, WT; Charles River #027, Kingston, NY, USA) and grown in Dulbecco's Modified Eagle Medium low-glucose culture media (Invitrogen #11885-084, Grand Island, NY, USA) supplemented with endothelial cell growth factors (Millipore #E2759-5, St-Louis, MO, USA), 10 % heat-inactivated fetal bovine serum (FBShi; Invitrogen #16000-044, Grand Island, NY, USA), 10 % heat-inactivated newborn calf serum (Invitrogen #16010-159, Grand Island, NY, USA), heparin (6300 USP Unit; Sandoz #02303108, Boucherville, QC, Canada), 1 % penicillin-streptomycin (Wisent #450-201-EL, St-Jean-Baptiste, QC, Canada), and 1 % fungizone (Wisent #450-105-QL, St-Jean-Baptiste, QC, Canada). To generate conditioned medium, mECs were exposed to serum-free medium (RPMI-1640; Life technologies #11875-119, Paisley, UK) for 9h. Quantification of apoptosis and necrosis was done as described [13,16]. Briefly, Hoechst 33342 (2′-(4-ethoxyphenyl)-5-(4-methyl-1-piperazinyl)-2.5′-bi-1H-benzimidazole, HO; Sigma Aldrich #B2261-25 MG, Oakville, ON, Canada) was used to identify apoptotic cells and propidium iodide (PI; Invitrogen #P3566, Grand Island, NY, USA) was used to label necrotic cells.

2.2. Preparation of extracellular vesicles

Serum-free medium conditioned with mECs was fractionated by sequential centrifugation, which included a 15-min centrifugation at 1200×*g* and 4 °C to pellet cell debris, followed by another 15-min centrifugation at 50,000×*g* and 4 °C to pellet apoptotic bodies (ApoBodies), and an 18-h ultracentrifugation at 200,000×*g* and 4 °C to pellet ApoExos. The pellets containing ApoBodies and ApoExos were resuspended in half of the initial volume of phosphate-buffered saline (D-PBS 1X; Wisent #311–430 CL, St-Jean-Baptiste, QC, Canada). Apoptosis and necrosis levels were assessed using HO and PI as described [13]. Protein concentration was assessed using the BCA microassay kit (Thermo Fisher #23235, Waltham, MA, USA) while proteasome caspase-like activity assay kit (Promega #G8641, Madison, WI, USA) was used to assess proteasome activity, both according to manufacturer instructions. Increased levels of LG3 and 20S proteasome in ApoExos compared to apoptotic bodies was showed by western blot as previously described [13].

2.3. Animal studies

Adult female WT mice (6–8 weeks; Charles River #027, Kingston, NY, USA), and TCR delta−/− (TCRγδ^{KO}) mice (B6.129P2-Tcrdtm1Mom/J; Hébert Laboratory, CRCHUM, QC, Canada) were maintained on a 12-h light-dark cycle and were fed with a normal diet *ad libitum*. All mice experiments were approved by CRCHUM's ethics review board. Mice were anesthetized with 2 % isoflurane inhalation and sacrificed by either cardiac puncture (to harvest blood) or cervical dislocation (to harvest cells in the peritoneal cavity without contaminating it with blood, as previously described) [16]. The spleen was harvested in complete medium in all experiments.

2.4. Injection of murine apoptotic endothelial membrane vesicles (ApoExos)

Using an established protocol, the mice received a 150 μl intravenous injection of the ApoExos preparation or the vehicle (D-PBS 1X) through the caudal vein every other day over three weeks, up to 8 injections in the different animal models used (see Animal studies section before) [15]. Twenty-one days after the first injection, the sera or peritoneal cavity cells and the spleen were harvested [13,16].

2.5. Cell isolation and In vitro stimulation of splenocytes or peritoneal cavity cells with TLR agonists

Cells were isolated from the spleen or the peritoneal cavity as previously described [16]. Briefly, the spleen was harvested in RPMI-1640 medium supplemented with L-glutamine, 10 % FBShi, and 1 % penicillin-streptomycin. The peritoneal cavity cells were harvested with 10 mL of cold D-PBS 1X medium supplemented with 3 % FBShi, as previously described [16,27]. Erythrocytes were lyzed with ammonium-chloride-potassium lysis buffer (Life technologies #A1049201, Grand Island, NY, USA), and B cells were isolated from splenocytes with an Easysep mouse pan-B cell isolation kit (STEMCELL technologies #19844, Vancouver, BC, Canada) according to manufacturer instructions. 2.5x10^6 cells (including splenocytes, B cells from splenocytes, or all cells from the peritoneal cavity) were cultured with TLR agonists for 3 days at 37 °C in a humidified atmosphere containing 5 % CO_2. The supernatants were harvested and stored at −80 °C until tested. The TLR agonists used to stimulate cells are listed in Table S1, and their concentration was derived from the literature: Pam3CSK4 for the TLR1/2 heterodimer, Poly (I:C) high or low molecular weight for TLR3, lipopolysaccharide (LPS) for TLR4, Flagellin (FLA) for TLR5, imiquimod for TLR7, and ODN2395 for TLR9.

2.6. Flow cytometry analyses for splenic germinal center B cells, follicular helper T cells and B1 cells

Single-cell suspensions from the spleen or peritoneal cavity were prepared and stained immediately for flow cytometry. A flow cytometer (FORTESSA, Becton Dickinson, Missisauga, ON, Canada) was used to determine the percentage of CD4+/programmed cell death protein 1 (PD-1)+/CXCR5+ follicular helper T cells among viable CD4$^+$ splenocytes [13,28,29]. The same flow cytometer was used to determine the percentage of CD45R+/GL-7+/CD95+ germinal center B cells among viable CD45R + B cells isolated from splenocytes [13,30,31]. Finally, another flow cytometer (LSRIIA, Becton Dickinson, Missisauga, ON, Canada) was used to determine the percentage of CD45R^{low}/CD19+/CD23- B1 cells among viable CD45R^{low}/CD19+ splenocytes. Monoclonal anti-mouse antibodies used are detailed in Table S2. All cytometry data were analyzed using the software FlowJo (version 10.7.1 or newer) (Fig. S3).

2.7. Assessment of circulating levels of total IgGs, ANA, anti–dsDNA, anti-AT1R, anti-perlecan/LG3, anti-vimentin, and anti-fibronectin

Antinuclear antibodies (ANA) levels were assessed using ANA mouse bioassay kits (USBiologicals, Swampscott, MA, USA); total IgG levels were assessed with mouse IgG Total Ready-SET-Go kits (Affimetrix, Vienna, Austria); anti-double strand DNA (anti-dsDNA) levels were assessed with anti-dsDNA mouse ELISA kits (BioVendor, Neuss, Deutschland); and the levels of angiotensin 1 receptor antibodies (anti-AT1R) were assessed with BioAssay™ ELISA Kits, mouse (USBiological, Salem, MA, USA), all in accordance with the manufacturers' instructions.

Serum levels of anti-Smith/nuclear ribonucleoprotein (Sm/nRNP), anti-Sm, anti-SSA (Ro), anti-SSB (La), anti-cardiolipin (CL) and anti-β2-glycoprotein I (β2GPI) were determined by ELISA, as described previously [32,33].

Anti-LG3, anti-vimentin, and anti-fibronectin titers were measured with an in-house ELISA. The recombinant perlecan fragment LG3 was produced and purified as previously described [13,34]. The first step of the ELISA was to coat 96-well Immulon II HB plates (ThermoFisher, Naperville, IL, USA) with 0.5 μg per well recombinant mouse LG3, vimentin (Cloud-Clone Corp., Katy, TX, USA) or fibronectin (MyBioSource, San Diego, CA, USA). The sera were diluted 1:100 for all ELISAs except those for IgG2a (1:75) and IgA (1:25), and 100 μl were added to each well. The plates were washed, and bound immunoglobulin (Ig) were detected using horseradish peroxidase coupled with an anti-mouse IgG (Jackson Immuno Research, West Grove, PA, USA),IgM (Millipore, Billerica, MA, USA), IgG1, IgG2a, IgG2b, IgG2c or IgG3 (Southern Biotech, Birmingham, AL, USA). Catalogue number can be found in Table S3. The reactions were initiated with 100 μl of tetramethylbenzidine substrate (BD Biosciences, Franklin Lakes, NJ, USA) and stopped with 50 μl of 1M sulfuric acid. Absorbance was then measured at 450 nm with a spectrophotometer. Results are expressed as optical density (OD) multiplicated by 1000.

2.8. Microarray

Autoantibodies were profiled from mouse serum with a custom antigen microarray, as described by Chruscinski et al. [35]. Briefly, antigens were spotted in duplicate onto nitrocellulose coated slides (Maine Manufacturing, Sanford, ME, USA) using a VersArray Chipwriter Pro (Virtek, ON, Canada). Slides were incubated with mouse serum (diluted 1:100) and then probed with a Cy3 labelled goat anti-mouse IgG antibody (Jackson Immunoresearch, Westgrove, PA, USA) and a Cy5 labelled goat anti-mouse IgM antibody (Jackson Immunoresearch, Westgrove, PA, USA). Fluorescence was quantified using an Axon 4200A scanner (Molecular Devices, Sunnyvale, CA, USA). List of autoantigens tested can be found in Table S4.

The systemic autoimmune-associated antigen array (catalogue #PA001) from GeneCopoeia (Rockville, MD, USA) was used to explore circulating autoantibodies present in WT compare to TCRγδ^{KO} mice after ApoExos injections. List of autoantigen tested can be found in Table S5.

Results are presented using the open access website heatmapper.ca.

2.9. Multiplex luminex-based quantification of cytokines

25 μl of sera were analyzed using ProcartaPlex Mouse Cytokine & Chemokine Panel 1A (Invitrogen, Vienna, Austria) and ProcartaPlex Mouse BAFF Simplex (Invitrogen, Vienna, Austria) according to the manufacturer's instructions. Cytokine levels were quantified using the Luminex xMAP Technology and the Bio-Plex 200 System (Bio-Rad, Missisauga, ON, Canada), and data were analyzed using the Bio-Plex Manager Software version 6.0.0.617.

2.10. Kidney damage assessment

Kidneys were included in paraffine and a hematoxylin and eosin (H&E) staining was used to assess infiltration and tubular injury score. Kidney fibrosis was assessed using Picro Sirius Red Stain Kit, (Abcam #ab150681, Toronto, ON, Canada). Blood urea nitrogen (BUN) was assessed using QuantiChrom TM Urea Assay Kit (Bioassay System #DIUR-100, Hayward, CA, USA) while proteinuria was assessed using Chemstrip 10A, (Roche Diagnostics #11379208119 , Indianapolis, IN, USA).

2.11. Statistical analyses

Means ± standard errors of the mean (SEM) were derived from at least three independent experiments, unless otherwise specified. Biological data were compared using a Student's t-test. All statistical analyses were performed using Prism 8.1.0 (Prism-GraphPad software, Inc). P values of less than 0.05 were considered statistically significant. Microarray data were analyzed with a two-way Anova test (Prism-GraphPad software, Inc).

3. Results

3.1. ApoExos trigger a systemic humoral response to LG3

ApoExos are apoptotic vesicles that differ from apoptotic bodies (Fig. 1) [13]. In this model, and consistent with previous data, murine aortic endothelial cells conditioned in a serum starvation milieu undergo apoptosis, but not necrosis (Fig. 1a) [13,17,18]. Compared to apoptotic bodies, ApoExos isolated by serial centrifugation were enriched in the 20S subunit of the proteasome (Fig.1c), exhibited higher proteasome activity (Fig. 1b), and carried LG3 (Fig. 1c) [13–15,17,18,36]. Moreover, in healthy wild type (WT) mice, the injection of ApoExos — but not of apoptotic bodies nor vehicle — increased circulating levels of anti-LG3 IgG (Fig. 1d).

3.2. Stimulation of TLR 1/2, 4, 7 and 9 triggers the release of anti-LG3-specific autoantibodies by B cells isolated from the peritoneal cavity of healthy mice

B cells targeting the autoantigen LG3 (i.e., the 5' fragment of the proteoglycan perlecan) were previously found in the normal B cell repertoire of naïve WT mice and seemed particularly enriched in the peritoneal cavity [16]. Since TLR agonists stimulate autoimmune responses, we explored the role of TLRs in triggering anti-LG3 responses. B cells from the spleen or peritoneal cavity of healthy WT mice were isolated and stimulated *in vitro* for 3 days with TLR agonists (Table S1). Anti-LG3 IgM were secreted by peritoneal and to a lesser extent by splenic B cells upon stimulation with TLR1/2, TLR4, TLR7, and TLR9 agonists (all $p < 0.001$), but not upon stimulation with TLR3 and TLR5 agonists (Fig. 1e and S1). This profile supports the notion that the normal B cell repertoire has the potential to produce anti-LG3 autoantibodies when stimulated by inflammatory triggers such as TLR agonists [16].

Interestingly, ApoExos treatment ablated the *in vitro* production of anti-LG3 IgM upon stimulation with TLR1/2 agonists ($p = 0.0034$; Fig. 1f), TLR4 agonists ($p = 0.0004$; Fig. 1g), and TLR7 agonists ($p = 0.0278$; Fig. 1h). A similar trend was observed with TLR9 stimulation (Fig. 1i). Fewer immune cells were isolated from the peritoneal cavity of ApoExos-injected mice than vehicle-injected mice ($p = 0.0038$; Fig. 1j). Moreover, compared with cells from vehicle-injected mice, those from ApoExos-injected mice contained a higher proportion of B1 cells ($p = 0.0012$; Fig. 1k), splenic follicular T cells ($p = 0.0069$; Fig. 1m), and germinal center B cells ($p = 0.0151$; Fig. 1l). Altogether, these results suggest that LG3 humoral response exists in the normal repertoire and becomes systemic upon ApoExos treatment.

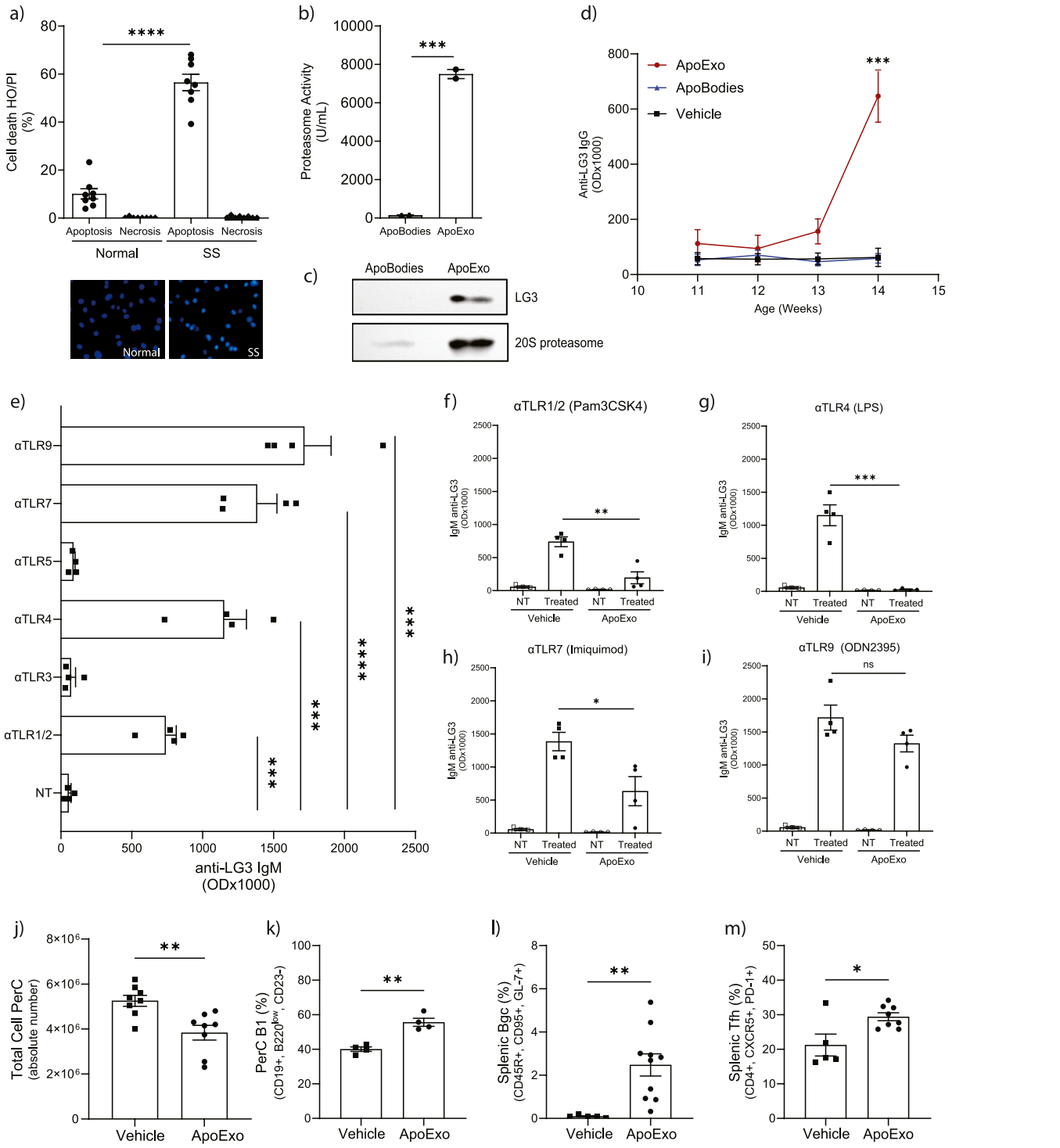

Fig. 1. B cells producing anti-LG3 are found in the normal B cell repertoire and are affected by ApoExos. (a) Levels of apoptosis (HO) or necrosis (PI) of murine aortic endothelial cells after 9 h in normal or serum starvation (SS) media. (b) Proteasome caspase-like activity assay kit revealed an increased proteasome activity in ApoExos compared to apoptotic bodies (ApoBodies). (c) Western blot showed increased in LG3 and 20S proteasome in ApoExos compare to ApoBodies. (d) ApoExos, but not ApoBodies or vehicle injections, produced anti-LG3 IgG autoantibodies ($p = 0.0001$). (e) LG3-specific B cells isolated from the peritoneal cavity (PerC) of vehicle-injected wild type (WT) mice are present in the normal repertoire and are activated in a TLR-dependent manner (TLR1/2, $p = 0.0001$; TLR4, $p = 0.0005$; TLR7, $p < 0.0001$; and TLR9, $p = 0.0001$) to secrete anti-LG3 IgM. ApoExos injection decreases anti-LG3 IgM production after stimulation with the aforementioned TLR agonists (TLR1/2, $p = 0.0034$ (f); TLR4, $p = 0.0004$ (g); TLR7, $p = 0.0278$ (h) and TLR9, trend only (i)) and in (j) total number of PerC cells compared to vehicle-injected WT mice ($p = 0.0038$). The percentage of (k) B1 cells among all B cells from the PerC, (l) splenic geminal center B cells (Bgc) and (m) follicular T cells (Tfh) increased after ApoExos injection (respectively, $p = 0.0012$, $p = 0.0069$ and $p = 0.0151$). Data are expressed as means ± SEMs, and statistical comparisons were carried out with a two-tailed Student's t-test. ****$p < 0.0001$; ***$p < 0.001$; **$p < 0.01$; *$p < 0.05$; OD, optical density; α, agonist.

3.3. ApoExos activate the IL-23/IL-17 autoimmune response

To further explore the impact of ApoExos injection, the sera of ApoExos- and vehicle-injected mice were analyzed by cytokine profiling using a 36-plex Luminex-based quantification assay. The results are expressed as ratios of circulating cytokine levels in ApoExos-versus vehicle-injected WT mice (Fig. 2a). Relative to vehicle-injected mice, ApoExos-injected mice exhibited lower circulating levels of the anti-inflammatory cytokine interleukin 10 (IL-10) ($p = 0.0027$; Fig. 2f); and increased circulating levels of IL-23 ($p = 0.0049$; Fig. 2b), IL-17 ($p = 0.0132$; Fig. 2c), CXCL-1 ($p = 0.0042$; Fig. 2d) and tumor necrosis factor alpha (TNF-α) ($p = 0.0249$; Fig. 2e), as shown by ELISA. Notably, the injection of apoptotic bodies did not trigger any response, which further highlights differences between those types of vesicles (Fig. S2).

3.4. ApoExos trigger the production of several autoantibodies in healthy mice

To further evaluate the systemic autoimmune response to ApoExos, the levels of circulating total IgG were assessed 21 days after the first injection. Total circulating IgG levels were higher in ApoExos-injected mice than vehicle-injected mice ($p = 0.0481$; Fig. 3a).

To assess the diversity and specificity of circulating autoantibodies produced upon ApoExos injection, serum autoantibodies were profiled using antigen microarrays with 155 antigens [37,38]. Unlike vehicle- and apoptotic bodies- injected mice, ApoExos-injected mice produced autoantibodies that were reminiscent of those found in classical systemic lupus erythematosus (SLE) (Fig. 3b and S4).

To confirm the antigen microarray results and further characterize the humoral autoimmunity triggered by ApoExos, we performed a serie of ELISAs to detect anti-LG3 antibodies, transplant-rejection-associated autoantibodies (i.e., anti-fibronectin [39,40], anti-vimentin [40–42] and anti-AT1R [40,43]), and hallmark SLE autoantibodies (i.e., ANA, anti-dsDNA, anti-Sm/nRNP, anti-Sm, anti-SSA [Ro], anti-SSB [La], anti-CL and anti-β2GPI) [44]. While the levels of autoantibodies associated with transplant rejection remained stable (Fig. 3I–m, n), those of anti-LG3 ($p = 0.0019$; Fig. 3c) and the aforementioned SLE-associated IgG autoantibodies increased in response to ApoExos ($p < 0.05$; Fig. 3d–k).

Overall, these observations demonstrate that ApoExos trigger an SLE-like systemic autoimmune humoral response in healthy WT mice.

Past studies showed an acceleration of vascular transplant rejection 21 days after the first injection of ApoExos [13]. However, our healthy mice with no other condition than ApoExos injection seem to keep relatively healthy kidney in the few days following the last injection (Fig. S5). Pathologist evaluation of kidney's H&E staining did not show significant differences between vehicle injected mice and ApoExos-injected ones in infiltration and tubular injury score 21 days after their first injection. Fig. S5c show representative example of staining for vehicle and ApoExos injected mice. We also confirmed that fibrosis was not significantly different between the control group and ApoExos injected mice with a Sirius red staining (Fig. S5c). ApoExos injected mice and vehicle injected ones also had similar levels of blood urea nitrogen (BUN) concentration (Fig. S5a) as well as negative urinary proteinuria (Fig. S5b). The interesting observations about the systemic autoimmune reaction that seems to occur leads us to the hypothesis that, while not sufficient to provoke injury of their own in the kidney, ApoExos are catalyzing harmful immune responses in context of

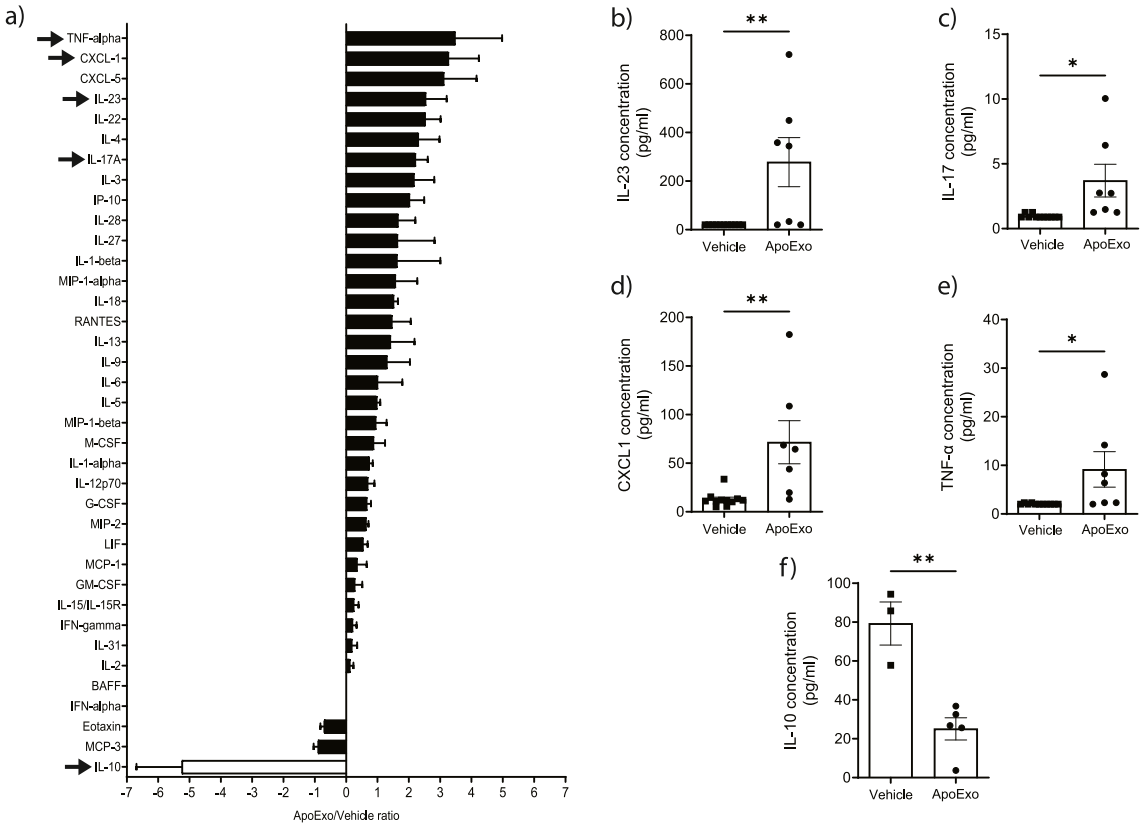

Fig. 2. ApoExos activate the IL-23/IL-17 autoimmune axis. (a) Ratio of cytokine levels in the sera of WT mice that received an ApoExos or vehicle injection, as measured by Luminex-based multiplex assay. (b) IL-23 ($p = 0.0049$), (c) IL-17 ($p = 0.0132$), (d) CXCL1 ($p = 0.0042$), (e) TNF-a ($p = 0.0249$), and (f) IL-10 ($p = 0.0027$) cytokines levels measured by ELISA in sera from WT mice after ApoExos or vehicle injection. Data were pooled from 3 independent experiments ($n = 6$ for each condition) and were expressed as means ± SEM. The statistical comparison between ApoExos and vehicle were carried out with a Student's t-test. ****$p < 0.0001$; ***$p < 0.001$; **$p < 0.01$; *$p < 0.05$.

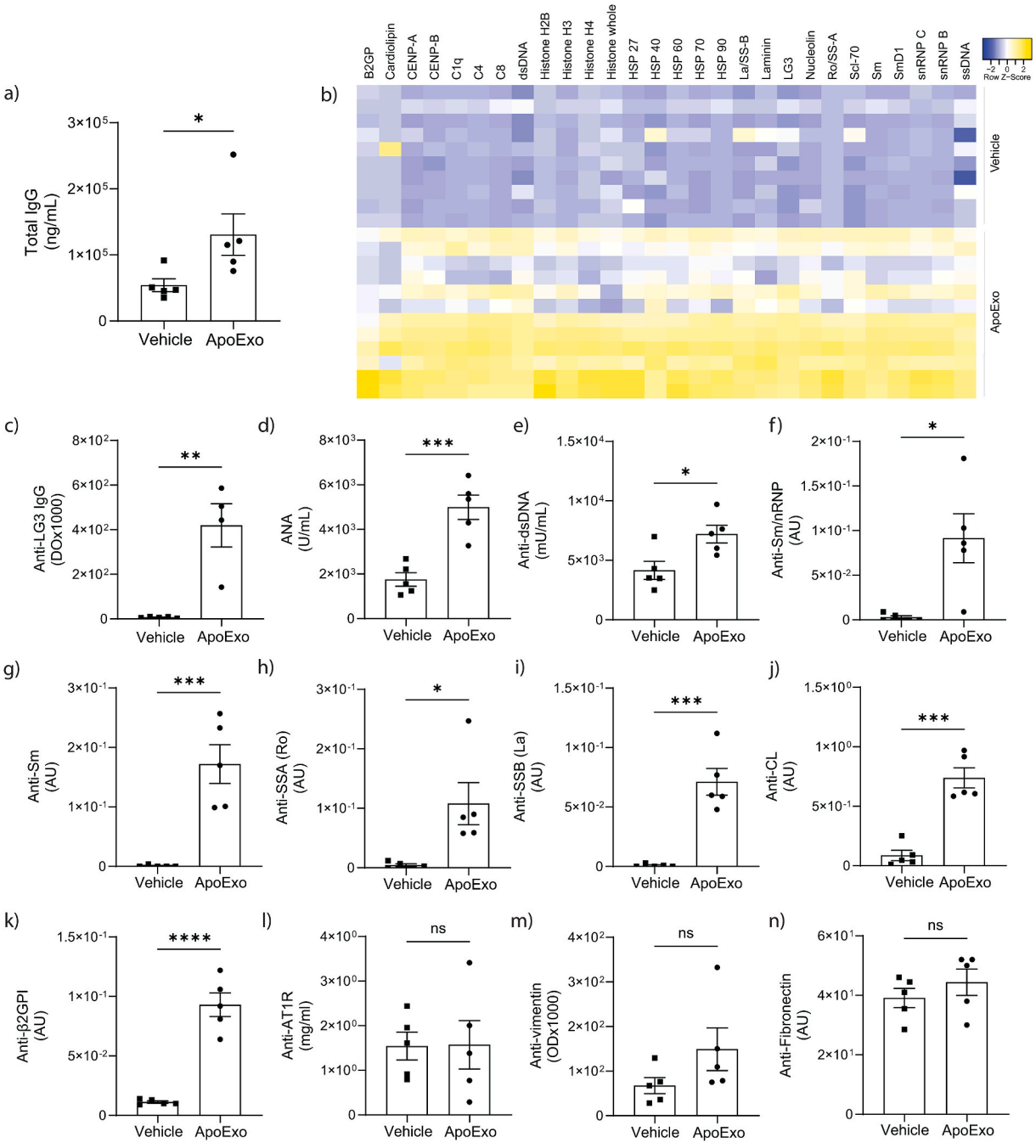

Fig. 3. ApoExos trigger the production of autoantibodies. (a) ELISA was performed on the sera from ApoExos- or vehicle-injected WT mice (n = 5), and a significant increase of circulating total IgG was observed (p=0.0481). (b) Microarray experiments of multiple autoantigens showed an SLE-associated autoantibody profile in mice injected with ApoExos, but not in those injected with vehicle. Autoantibodies detected were IgG. Each row of the heatmap represents one animal for a total of 12 ApoExos-injected WT mice and 10 vehicle-injected WT mice. The results were compared by ANOVA and minimal q value of represented data was 0,05. Blue and yellow are low and high level respectively. ELISA of sera from ApoExos- or vehicle-injected mice confirmed the increased levels of SLE-associated autoantibodies (i.e., (c) anti-LG3 (p=0.0019), (d) antinuclear antibodies (ANA) (p=0.0009), (e) anti-dsDNA (p=0.0212), (f) anti-Sm/nRNP (p=0.0124), (g) anti-Sm (p=0.0008), (h) anti-SSA (Ro) (p=0.0195), (i) anti-SSB (La) (p=0.0002), (j) anti-cardiolipin (CL) (p=0.0001) and (k) anti-β2GPI (p<0.0001)), while autoantibodies related to autoimmunity in transplantation were not affected (i.e., (l) anti-AT1R, (m) anti-vimentin and (n) anti-fibronectin). Statistical significance was assessed by Student's t-test. ****p < 0.0001; ***p < 0.001; **p < 0.01; *p < 0.05; ns not significant. Results are expressed as indicated: AU, Arbitrary Units; OD, Optical Density. (For interpretation of the references to colour in this figure legend, the reader is referred to the Web version of this article.)

vascular damage or in conditions were systemic inflammation is present.

3.5. γδT cells mediate anti-LG3 class switching after ApoExos injection

In a murine model of vascular rejection, *γδT* cells were previously shown to mediate the humoral response triggered by ApoExos [15]. Therefore, we examined the impact of ApoExos-induced humoral responses in TCRγδ knockout (KO) mice. Interestingly, unlike WT mice, these mice exhibited no increase of splenic germinal center B cells following ApoExos injection (p = 0.0027; Fig. 4a), suggesting γδT cells are involved in generating ApoExos-induced splenic germinal centers.

Using LG3-specific responses as a marker of the humoral response to

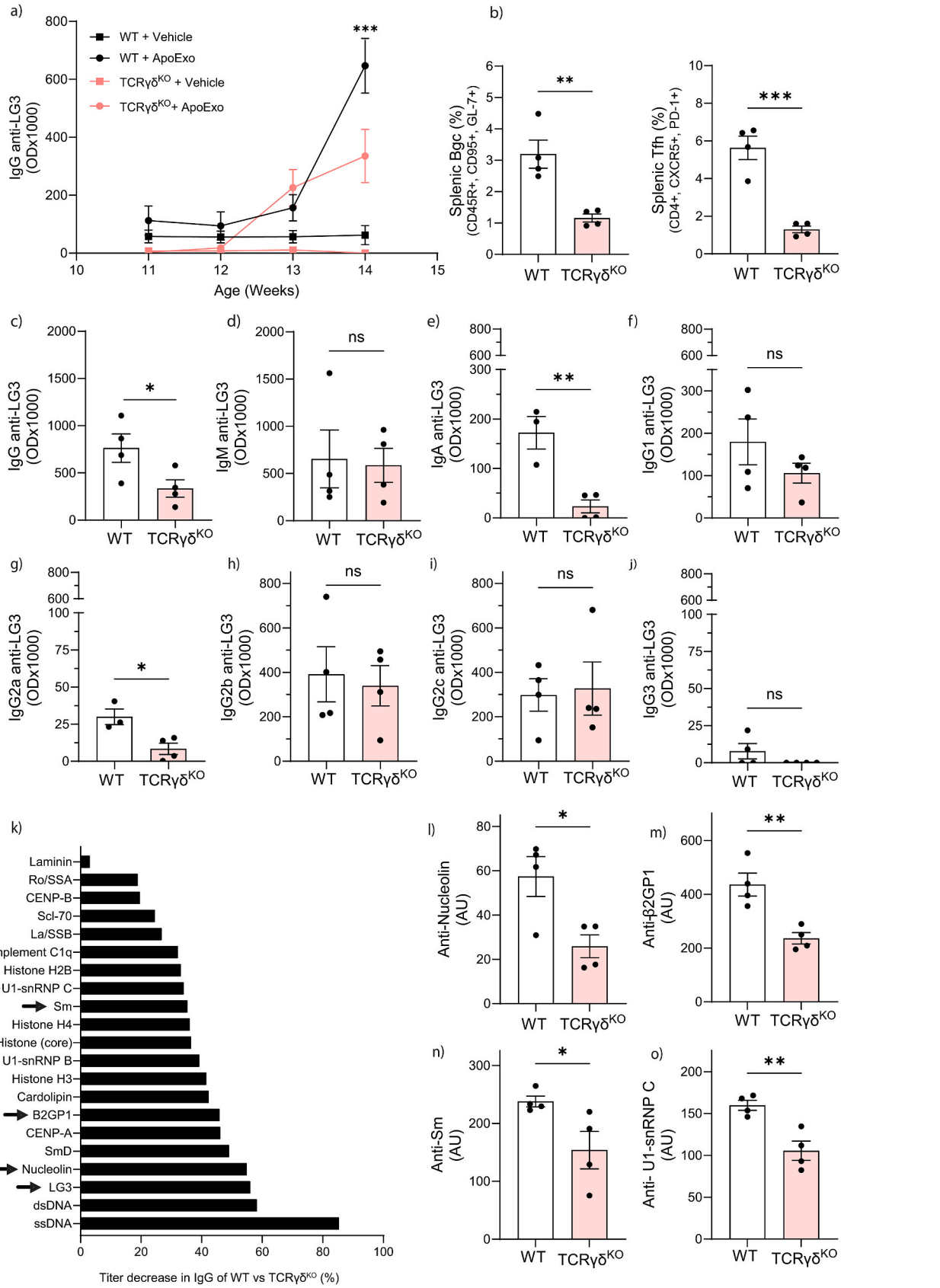

(caption on next page)

Fig. 4. γδT cells mediate anti-LG3 class switching after ApoExos injection. (a) TCRγδ^{KO} mice injected with ApoExos produce more circulating anti-LG3 IgG than those injected with the vehicle, although the levels remained below those of ApoExos-injected WT mice. (b) TCRγδ^{KO} mice injected with ApoExos have a decreased percentage of germinal center B cell (Bgc) and follicular helper T cell (Tfh) in total alive splenocytes harvested 21 days after the first exposure to ApoExos compared to WT mice also injected with ApoExos (respectivly p=0.0046 and p=0.0005). ELISA on serum from both strains injected with ApoExos showed unchanged levels of circulating anti-LG3 (d) IgM in the absence of γδT cells while (c) anti-LG3 IgG were significantly decreased (p = 0.05). (e) The levels of circulating anti-LG3 IgA were also significantly lower in TCRγδ^{KO} mice than WT ones after ApoExos injection (p = 0.005). An assessment of anti-LG3 IgG subclasses showed unchanged levels of (f) IgG1, (h) IgG2b, (i) IgG2c and (j) IgG3, while (g) IgG2a significantly decreased (p = 0.005). (k) Circulating autoantibodies from ApoExos injected in WT mice profiled using an antigen microarray and compared to the profile from ApoExos injected TCRγδ^{KO} mice. Arrows identify antibodies showing significant decrease that are also showed in independent graphs (l) anti-nucleolin (p=0.0229), (m) anti-β2GPI (p=0.0057), (n) anti-Sm (p=0.0466) and (o) anti-U1-sn-RNP (p=0.0057). Statistical significance was assessed by Student's t-test. ****p < 0.0001; ***p < 0.001; **p < 0.01; *p < 0.05; ns not significant. OD, Optical Density; AU, Arbitrary Unit.

ApoExos, we further characterized this humoral response in TCR$\gamma\delta^{KO}$ mice. Relative to WT mice, these mice exhibited similar levels of anti-LG3 IgM (p = 0.8558; Fig. 4d), but reduced levels of circulating IgG (p = 0.05; Fig. 4c).

Next, we characterized by ELISA the anti-LG3 IgG subclasses produced in response to ApoExos. In WT mice, ApoExos injection increased the levels of all anti-LG3 IgG subclasses (not shown). When comparing ApoExos-injected WT and TCR$\gamma\delta^{KO}$ mice, we observed similar levels of IgG1 (p = 0.2570; Fig. 4f), IgG2b (p = 0.7467; Fig. 4h), IgG2c (p = 0.8408; Fig. 4i), and IgG3 (0.1844; Fig. 4j). However, TCR$\gamma\delta^{KO}$ ApoExos-injected mice had reduced levels of IgG2a (p = 0.0190; Fig. 4g).

The levels of IgA, which is implicated in immune tolerance, were also evaluated. Interestingly, ApoExos injection increased IgA levels in WT, but not in TCR$\gamma\delta^{KO}$ mice (p = 0.0052; Fig. 4e).

Circulating autoantibodies from ApoExos injected TCRγδ^{KO} mice were profiled using an antigen microarray and compared to the profile from ApoExos injected WT mice. We found that relative to WT mice, TCRγδ^{KO} mice exhibit similar levels of IgM (not shown) autoantibodies, but reduced levels of circulating IgGs (Fig. 4k), although with a different amplitude, for most of the autoantibodies triggered by ApoExos in WT mice (Fig. 3b and 4k-o).

These results demonstrate the diversity and maturity of the humoral response triggered by ApoExos in healthy mice. γδT cells were also identified as key mediators of the maturation of the ApoExos-induced autoantibodies in healthy mice.

4. Discussion

The normal B cell repertoire includes at least some autoreactive B cells, and those self-ligands might be crucial for their clonal proliferation and persistence [2–4,6]. In this work, we confirmed that healthy mice exhibit self-reactive B cells targeting LG3/perlecan — an antigen packaged in ApoExos. We also demonstrate that specific TLR engagement can stimulate these clones *in vitro*. Moreover, the injection of ApoExos in healthy nonautoimmune mice triggers the expression of IL-23, IL-17, circulating LG3-specific autoantibodies, and SLE-associated autoantibodies. γδT cells were also identified as key mediators of the maturation of the ApoExos-induced humoral autoimmune responses in healthy mice.

Previous work in humans supported the presence of self-reactive, LG3/perlecan-specific clones in the normal B cell repertoire [12]. Humoral immune responses against LG3/perlecan have been found to be associated with graft rejection in cohort studies and animal models of acute and chronic allograft rejection [12,16,45]. In one study, LG3/perlecan-specific B cells were detected before transplantation in patients without any (known) autoimmune condition [12]. These autoimmune responses are suspected to have been caused by ischemia-reperfusion injury and inflammation, at least in part through the release of damage associated molecular patterns (DAMPS) such as TLR agonists. Here, we confirm the presence of LG3-specific B cells in the peritoneal cavity and to a lesser extend in the spleen of healthy animals, and find that specific TLR stimulation (i.e., 1/2, 4, 7, 9) *in vitro* stimulates the production of anti-LG3 autoantibodies. It will be important in future studies to evaluate the relative importance of different compartments such as the spleen and the peritoneal cavity in the response to ApoExos. There is also evidence that, in addition to autoantigens (e.g., LG3), ApoExos carry TLR agonists (e.g., heat shock proteins [HSP] 75, 10, 71, and 70, fibronectin, and PAI-1 [SERPINE 1] [13]) that initiate these autoimmune responses *in vivo*. Perlecan fragments were also reported to bind TLR2 and TLR4 [46]. Importantly, using an unbiased deep RNA sequencing approach, ApoExos were shown to have a distinct transcriptomic profile and carry RNA sequences exhibiting immunostimulatory potential, including mitochondrial transfer RNAs, U1 small nuclear RNA, pathogen-like endogenous retroelements, and Poly-U, AU- and GU-rich motifs [14]. RNA structure modeling also revealed that ApoExos, compared to apoptotic bodies, display an abundance of unstably folded RNA sequences which are prone to generate single-stranded structures — the preferred ligands of endosomal TLRs, such as TLR7, 8 and 9 [14].

Hence, ApoExos contain a diversified repertoire of immunostimulatory proteins and self RNAs that can trigger autoimmunity.

Previous findings from our group demonstrated the role of γδT cells in coordinating autoimmune responses triggered by ApoExos after transplantation. Indeed, in a murine model of vascular rejection, γδT cell invalidation abrogated the ApoExos-induced production of circulating autoantibodies and formation of tertiary lymphoid organ formation within vascular allografts [15]. The present report highlights the importance of γδT cells in sensing ApoExos-dependent autoimmune signals in healthy mice. Compared to WT mice, TCRγδ^{KO} mice showed an impaired accumulation of germinal center B cells in the spleen upon ApoExos injection, suggesting a role for γδT cells in the formation of germinal centers in response to ApoExos. Since class-switching occurs in germinal centers [47], we looked at antibody maturation following ApoExos injection in TCRγδ^{KO} mice. While autoantibodies IgM levels remained elevated after ApoExos injection in both TCRγδ^{KO} and WT mice, the absence of γδT cells reduced the production of autoantibodies in response to ApoExos. Using anti-LG3 as a marker of antibody maturation following ApoExos injection we also found that the absence of γδT cells impaired the production of anti-LG3 IgA and IgG (particularly IgG2a) in response to ApoExos. Collectively, these observations suggest a role for γδT cells in autoantibody maturation in response to ApoExos.

These observations raise several questions. First, in contrast to conventional T lymphocytes, γδT cells can be activated without a cognate TCR ligand [48]. In future investigations, it will be interesting to study whether the activation of γδT cells by ApoExos is antigen-specific or stems from signaling pathways triggered by TLR agonists or non-protein mediators. Second, the implication of ApoExos-triggered class switch of anti-LG3 antibodies drives the response towards specific effector functions [49]. Here, we show that ApoExos promote the switch of anti-LG3 Ig to IgG2a, the subtype with the highest affinity for C1q [50], which is key to activating the complement system. In line with our observations, we previously showed that inflammation promotes a class switch that enables the fixing of complement subclasses in naïve WT mice [16]. We also showed that complement-fixing anti-LG3 IgG were associated with acute vascular rejection in kidney transplant patients [12]. These observations suggest that ApoExos trigger the production of complement-fixing autoantibodies, and that γδT cells are key modulators of this response. Further studies will be key to unravel implications of the γδT cells dependent antibodies maturation on the pathogenicity of ApoExos triggered humoral responses.

IgG subclasses also interact with Fcγ receptors (FcγRs) to induce effector responses, such as antibody-dependant cellular cytotoxicity, the clearance of opsonized particles, and the release of inflammatory mediators [51,52]. Because activating (FcγRI, FcγRIII and FcγRIV) and inhibitory (FcγRIIB) FcγRs are usually co-expressed, the outcome of IgG binding depends on the relative affinity of an antibody for its receptor, which can be expressed as an activating-to-inhibitory (A/I) ratio [53]. IgG2a has the highest A/I ratio, indicating an ability to induce pathogenic reactions [31].

In SLE, the loss of immune tolerance generates autoantibodies that accumulate in organs. IgG2a autoantibodies are the most pathogenic isotypes as they recruit FcγRIV-expressing macrophages [54]. Similar to our observation, the class switching (but not the development) of IgM anti-self B cells to these pathogenic subclasses requires TLR9 and MyD88. Their absence thwarts the class switching of autoreactive B cells to IgG2a, thus reducing SLE activity and mortality [54]. Importantly, TLR7 ligands also drive the activation and class switching of autoreactive transitional B cells [55]. Our data suggest that ApoExos released upon vascular injury activate γδT cells, since TLR signaling leads to autoantibody class switch to Ig isotypes involved in autoimmune diseases. In future studies, TLR KO mice may prove useful to evaluate the role of the different TLRs in the maturation of the autoimmune response driven by ApoExos. Since vascular injury is a common feature of SLE, future investigations should focus on characterizing the role of vascular injury-derived ApoExos in the humoral autoimmune response of this disease.

ApoExos also triggered a class switch of anti-LG3 autoantibodies to IgA. IgA is generally considered a non-inflammatory antibody and is chiefly involved in mucosal immunity [56,57]. Yet IgA autoantibodies are suspected to be involved in several diseases, such as IgA nephropathy [58,59], IgA vasculitis [60], rheumatoid arthritis [61] and multiple sclerosis [62]. However, the role of IgA autoantibodies in these diseases and the mechanisms that control their production remain ill-defined. Based on our data, the study of immune responses to vascular injury-derived ApoExos might provide valuable insights about the pathophysiological mechanisms of these diseases.

5. Conclusion

We conclude that ApoExos display immune mediating functions that can stimulate B cells in the normal repertoire and drive them to release multiple autoantibodies. TLR activation and γδT cells were also identified as key modulators of this ApoExos-induced humoral autoimmune response. Future investigation should address the role of these vascular injury-derived immune responses in immune homeostasis and pathogenesis.

Funding

The authors acknowledge support from the Canadian Institutes of Health Research (CIHR) MOP-15447, PJT-148884 (MJH); PJT-180278 (MD); PJT-159652 (JR); and CIHR scholarship (SJ), the Kidney Foundation of Canada (MD) and Natural Sciences and Engineering Research Council (NSERC) RGPIN-2021-03004 (MD). MJH is the co-holder of the Shire Chair in Nephrology, Transplantation and Renal Regeneration of the Université de Montréal. We thank the J.-L. Lévesque Foundation for renewed support.

CRediT authorship contribution statement

Sandrine Juillard: Writing – original draft, Validation, Methodology, Investigation, Formal analysis, Data curation. **Annie Karakeussian-Rimbaud:** Resources, Methodology, Formal analysis, Data curation. **Marie-Hélène Normand:** Writing – review & editing, Methodology, Investigation, Data curation. **Julie Turgeon:** Writing – review & editing, Methodology, Investigation, Data curation. **Charlotte Veilleux-Trinh:** Writing – review & editing, Methodology, Investigation, Data curation. **Alexa C. Robitaille:** Writing – review & editing, Methodology, Data curation. **Joyce Rauch:** Writing – review & editing, Methodology, Funding acquisition, Data curation. **Andrzej Chruscinski:** Writing – review & editing, Methodology, Data curation. **Nathalie Grandvaux:** Writing – review & editing, Methodology, Data curation. **Éric Boilard:** Writing – review & editing, Methodology, Data curation. **Marie-Josée Hébert:** Writing – review & editing, Validation, Project administration, Methodology, Investigation, Funding acquisition, Conceptualization. **Mélanie Dieudé:** Writing – original draft, Validation, Project administration, Methodology, Investigation, Funding acquisition, Formal analysis, Conceptualization.

Declaration of competing interest

The authors declare that they have no known competing financial interests or personal relationships that could have appeared to influence the work reported in this paper.

Data availability

Data will be made available on request.

Acknowledgements

The authors acknowledge the support of the CRCHUM platforms, namely, the animal facility and its team, and the flow cytometry platform. We also thank Rebecca Subang from Dr. Rauch laboratory for technical assistance.

Appendix A. Supplementary data

Supplementary data to this article can be found online at https://doi.org/10.1016/j.jtauto.2024.100250.

References

[1] S. Avrameas, et al., Naturally occurring B-cell autoreactivity: a critical overview, J. Autoimmun. 29 (4) (2007) 213–218.
[2] J. Palma, et al., Natural antibodies - facts known and unknown, Cent. Eur. J. Immunol. 43 (4) (2018) 466–475.
[3] N. Baumgarth, B-1 cell heterogeneity and the regulation of natural and antigen-induced IgM production, Front. Immunol. 7 (2016) 324.
[4] N. Baumgarth, The double life of a B-1 cell: self-reactivity selects for protective effector functions, Nat. Rev. Immunol. 11 (1) (2011) 34–46.
[5] N. Baumgarth, A hard(y) look at B-1 cell development and function, J. Immunol. 199 (10) (2017) 3387–3394.
[6] H.U. Lutz, Naturally occurring antibodies, Adv. Exp. Med. Biol. 750 (2012) vii–x.
[7] S. Arandjelovic, K.S. Ravichandran, Phagocytosis of apoptotic cells in homeostasis, Nat. Immunol. 16 (9) (2015) 907–917.
[8] H.U. Lutz, Homeostatic roles of naturally occurring antibodies: an overview, J. Autoimmun. 29 (4) (2007) 287–294.
[9] X. Xu, Y. Lai, Z.C. Hua, Apoptosis and apoptotic body: disease message and therapeutic target potentials, Biosci. Rep. 39 (1) (2019).
[10] Z.X. Xiao, J.S. Miller, S.G. Zheng, An updated advance of autoantibodies in autoimmune diseases, Autoimmun. Rev. 20 (2) (2021) 102743.
[11] J.S. Navratil, J.M. Ahearn, Apoptosis, clearance mechanisms, and the development of systemic lupus erythematosus, Curr. Rheumatol. Rep. 3 (3) (2001) 191–198.
[12] H. Cardinal, et al., Antiperlecan antibodies are novel accelerators of immune-mediated vascular injury, Am. J. Transplant. 13 (4) (2013) 861–874.
[13] M. Dieude, et al., The 20S proteasome core, active within apoptotic exosome-like vesicles, induces autoantibody production and accelerates rejection, Sci. Transl. Med. 7 (318) (2015) 318ra200.
[14] M.P. Hardy, et al., Apoptotic endothelial cells release small extracellular vesicles loaded with immunostimulatory viral-like RNAs, Sci. Rep. 9 (1) (2019) 7203.
[15] M. Dieude, et al., Extracellular vesicles derived from injured vascular tissue promote the formation of tertiary lymphoid structures in vascular allografts, Am. J. Transplant. 20 (3) (2020) 726–738.
[16] L. Padet, et al., New insights into immune mechanisms of antiperlecan/LG3 antibody production: importance of T cells and innate B1 cells, Am. J. Transplant. 19 (3) (2019) 699–712.
[17] A. Brodeur, et al., Apoptotic exosome-like vesicles transfer specific and functional mRNAs to endothelial cells by phosphatidylserine-dependent macropinocytosis, Cell Death Dis. 14 (7) (2023) 449.

[18] D. Beillevaire, et al., Autolysosomes and caspase-3 control the biogenesis and release of immunogenic apoptotic exosomes, Cell Death Dis. 13 (2) (2022) 145.
[19] G.J. Brown, et al., TLR7 gain-of-function genetic variation causes human lupus, Nature 605 (7909) (2022) 349–356.
[20] S. Fillatreau, B. Manfroi, T. Dörner, Toll-like receptor signalling in B cells during systemic lupus erythematosus, Nat. Rev. Rheumatol. 17 (2) (2021) 98–108.
[21] M.A. Masum, et al., Induced expression of Toll-like receptor 9 in peritubular capillary endothelium correlates with the progression of tubulointerstitial lesions in autoimmune disease-prone mice, Lupus 28 (3) (2019) 324–333.
[22] K. Ma, et al., Roles of B Cell-Intrinsic TLR signals in systemic lupus erythematosus, International Jornal of Molecular Science 16 (2015) 22.
[23] Y. Murakami, et al., Anti-TLR7 antibody protects against lupus nephritis in NZBWF1 mice by targeting B cells and patrolling monocytes, Front. Immunol. 12 (2021) 777197.
[24] S.A. Jenks, et al., Distinct effector B cells induced by unregulated toll-like receptor 7 contribute to pathogenic responses in systemic lupus erythematosus, Immunity 49 (4) (2018) 725–739 e6.
[25] T. Wang, et al., High TLR7 expression drives the expansion of CD19(+)CD24(hi) CD38(hi) transitional B cells and autoantibody production in SLE patients, Front. Immunol. 10 (2019) 1243.
[26] N. Elloumi, et al., Relevant genetic polymorphisms and kidney expression of Toll-like receptor (TLR)-5 and TLR-9 in lupus nephritis, Clin. Exp. Immunol. 190 (3) (2017) 328–339.
[27] A. Ray, B.N. Dittel, Isolation of mouse peritoneal cavity cells, J. Vis. Exp. (35) (2010).
[28] G. Cao, et al., CD4+CXCR5+PD-1+ T follicular helper cells play a pivotal role in the development of rheumatoid arthritis, Med Sci Monit 25 (2019) 3032–3040.
[29] Y. Cai, et al., The frequency of intrathyroidal follicular helper T cells varies with the progression of graves' disease and hashimoto's thyroiditis, J Immunol Res 2022 (2022) 4075522.
[30] P. Ramezani-Rad, R.C. Rickert, Quick and easy purification of murine untouched naive B cells or germinal center B cells by MACS, STAR Protoc 2 (1) (2021) 100369.
[31] P. Ramezani-Rad, et al., Cyclin D3 governs clonal expansion of dark zone germinal center B cells, Cell Rep. 33 (7) (2020) 108403.
[32] J.S. Levine, et al., Immunization with an apoptotic cell-binding protein recapitulates the nephritis and sequential autoantibody emergence of systemic lupus erythematosus, J. Immunol. 177 (9) (2006) 6504–6516.
[33] D. Salem, et al., beta2-Glycoprotein I-specific T cells are associated with epitope spread to lupus-related autoantibodies, J. Biol. Chem. 290 (9) (2015) 5543–5555.
[34] M. Soulez, et al., Epidermal growth factor and perlecan fragments produced by apoptotic endothelial cells co-ordinately activate ERK1/2-dependent antiapoptotic pathways in mesenchymal stem cells, Stem Cell. 28 (4) (2010) 810–820.
[35] A. Chruscinski, et al., Generation of antigen microarrays to screen for autoantibodies in heart failure and heart transplantation, PLoS One 11 (3) (2016) e0151224.
[36] F. Migneault, et al., Apoptotic exosome-like vesicles regulate endothelial gene expression, inflammatory signaling, and function through the NF-kappaB signaling pathway, Sci. Rep. 10 (1) (2020) 12562.
[37] L. Grosman-Rimon, et al., Increases in serum autoantibodies after left ventricular assist device implantation, J. Card. Fail. 25 (4) (2019) 301–306.
[38] A. Chruscinski, et al., Generation of two-color antigen microarrays for the simultaneous detection of IgG and IgM autoantibodies, J. Vis. Exp. (2016) 115.
[39] N. Angaswamy, et al., Immune responses to collagen-IV and fibronectin in renal transplant recipients with transplant glomerulopathy, Am. J. Transplant. 14 (3) (2014) 685–693.
[40] S. Clotet-Freixas, et al., Increased autoantibodies against ro/SS-A, CENP-B, and La/SS-B in patients with kidney allograft antibody-mediated rejection, Transplant Direct 7 (10) (2021) e768.
[41] T. Divanyan, et al., Anti-vimentin antibodies in transplant and disease, Hum. Immunol. 80 (8) (2019) 602–607.
[42] M.L. Rose, Role of anti-vimentin antibodies in allograft rejection, Hum. Immunol. 74 (11) (2013) 1459–1462.
[43] M.H. Pearl, et al., Angiotensin II Type 1 receptor antibodies are associated with inflammatory cytokines and poor clinical outcomes in pediatric kidney transplantation, Kidney Int. 93 (1) (2018) 260–269.
[44] D. Accapezzato, et al., Advances in the pathogenesis and treatment of systemic lupus erythematosus, Int. J. Mol. Sci. 24 (7) (2023).
[45] M. Dieudé, H. Cardinal, M.J. Hébert, Injury derived autoimmunity: anti-perlecan/LG3 antibodies in transplantation, Hum. Immunol. 80 (8) (2019) 608–613.
[46] L. Schaefer, Complexity of danger: the diverse nature of damage-associated molecular patterns, J. Biol. Chem. 289 (51) (2014) 35237–35245.
[47] N.S. De Silva, U. Klein, Dynamics of B cells in germinal centres, Nat. Rev. Immunol. 15 (3) (2015) 137–148.
[48] S. Paul, et al., Phenotypic and functional plasticity of gamma-delta (γδ) T cells in inflammation and tolerance, Int. Rev. Immunol. 33 (6) (2014) 537–558.
[49] G.D. Victora, M.C. Nussenzweig, Germinal centers, Annu. Rev. Immunol. 30 (2012) 429–457.
[50] J.M. Chemouny, et al., Protective role of mouse IgG1 in cryoglobulinaemia; insights from an animal model and relevance to human pathology, Nephrol. Dial. Transplant. 31 (8) (2016) 1235–1242.
[51] X. Chen, et al., Immunoglobulin G subclasses confer protection against Staphylococcus aureus bloodstream dissemination through distinct mechanisms in mouse models, Proc Natl Acad Sci U S A 120 (14) (2023) e2220765120.
[52] F. Nimmerjahn, et al., FcgammaRIV: a novel FcR with distinct IgG subclass specificity, Immunity 23 (1) (2005) 41–51.
[53] N. Vukovic, et al., Isotype selection for antibody-based cancer therapy, Clin. Exp. Immunol. 203 (3) (2021) 351–365.
[54] M. Ehlers, et al., TLR9/MyD88 signaling is required for class switching to pathogenic IgG2a and 2b autoantibodies in SLE, J. Exp. Med. 203 (3) (2006) 553–561.
[55] S.W. Du, et al., Integrated B cell, toll-like, and BAFF receptor signals promote autoantibody production by transitional B cells, J. Immunol. 201 (11) (2018) 3258–3268.
[56] O. Pabst, E. Slack, IgA and the intestinal microbiota: the importance of being specific, Mucosal Immunol. 13 (1) (2020) 12–21.
[57] K.E. Huus, C. Petersen, B.B. Finlay, Diversity and dynamism of IgA-microbiota interactions, Nat. Rev. Immunol. 21 (8) (2021) 514–525.
[58] Q. Sun, et al., Aberrant IgA1 glycosylation in IgA nephropathy: a systematic review, PLoS One 11 (11) (2016) e0166700.
[59] P. Launay, et al., Fcalpha receptor (CD89) mediates the development of immunoglobulin A (IgA) nephropathy (Berger's disease). Evidence for pathogenic soluble receptor-Iga complexes in patients and CD89 transgenic mice, J. Exp. Med. 191 (11) (2000) 1999–2009.
[60] M.H. Heineke, et al., New insights in the pathogenesis of immunoglobulin A vasculitis (Henoch-Schönlein purpura), Autoimmun. Rev. 16 (12) (2017) 1246–1253.
[61] C. Jorgensen, et al., IgA isotype rheumatoid factor in rheumatoid arthritis: clinical implications, Clin. Exp. Rheumatol. 14 (3) (1996) 301–304.
[62] J. Kroth, et al., Increased cerebrospinal fluid albumin and immunoglobulin A fractions forecast cortical atrophy and longitudinal functional deterioration in relapsing-remitting multiple sclerosis, Mult. Scler. 25 (3) (2019) 338–343.